PREPRINT UCRL-79655

CONF-771102--16

Lawrence Livermore Laboratory

A FLUORESCENCE-PUMPED PHOTOLYTIC GAS LASER SYSTEM FOR A COMMERCIAL LASER FUSION POWER PLANT

Michael J. Monsler

MASTER

July 14, 1977

This paper was prepared for submission to the American Institute of Chemical Engineers Conference on November 13-17, 1977 in New York.

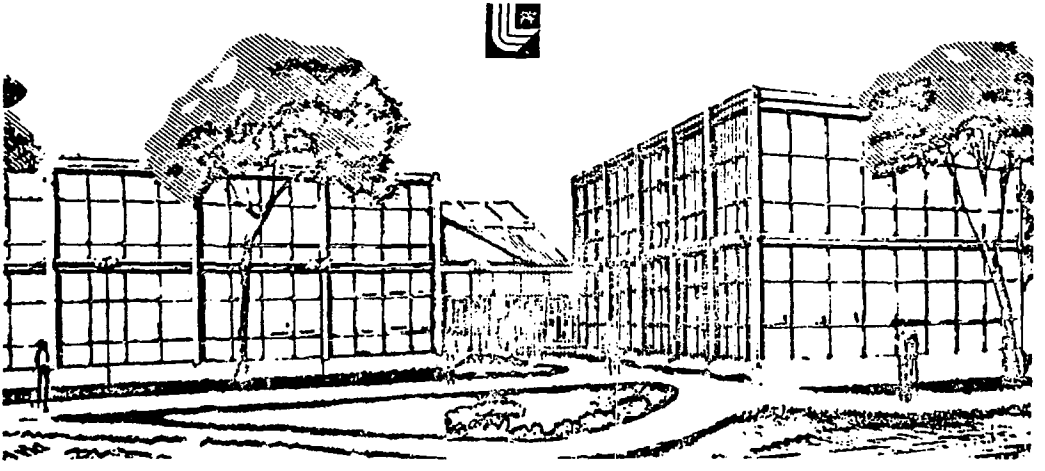

A FLUORESCENCE-PUMPED PHOTOLYTIC GAS LASER SYSTEM FOR A COMMERCIAL LASER FUSION POWER PLANT*

Michael J. Monsler

Lawrence Livermore Laboratory
University of California
Livermore, California

Abstract

The first results are given for the conceptual design of a short-wavelength gas laser system suitable for use as a driver (high average power ignition source) for a commercial laser fusion power plant. A comparison of projected overall system efficiencies of photolytically excited oxygen, sulfur, selenium and iodine lasers is described, using a unique windowless laser cavity geometry which will allow scaling of single amplifier modules to 125 kJ per aperture for 1 ns pulses. On the basis of highest projected overall efficiency, a selenium laser is chosen for a conceptual power plant fusion laser system. This laser operates on the 489 nm transauroral transition of selenium, excited by photolytic

*Work performed under the auspices of U.S. Energy Research & Development Administration under Contract W7405-ENG-48.

dissociation of COSe by ultraviolet fluorescence radiation. Power balances and relative costs for optics, electrical power conditioning and flow conditioning of both the laser and fluorescer gas streams are discussed for a system with the following characteristics: 8 operating modules, 2 standby modules, 125 kJ per module, 1.4 pulses per second, 1.4 MW total average power. The technical issues of scaling visible and near-infrared photolytic gas laser systems to this size are discussed.

A FLUORESCENCE-PUMPED PHOTOLYTIC GAS LASER SYSTEM FOR A COMMERCIAL LASER FUSION POWER PLANT

Introduction

A preliminary conceptual design is presented for a short wavelength, high energy, high average power gas laser system for a commercial laser fusion power plant. It is part of a study being performed at Lawrence Livermore Laboratory to exploit recent breakthroughs in high gain target design which have significantly relaxed requirements on the fusion laser system.[1] A previous study[2] also used a photolytic (oxygen) laser system as a basis for a commercial power plant; this present study considers a different range of operating parameters and offers more concrete estimates of efficiencies and sizes.

It has long been recognized at LLL that laser-induced fusion can be approached using many different target concepts which, in terms of projected applications, dictate a range of laser-system performance requirements. On the basis of extensive computation and experiments conducted to date, in addition to the economic and system constraints, we have established preliminary laser system performance requirements for commercial electric power production. The nominal requirements are summarized below.

• Wavelength	250-2000 nm
• Pulse duration	$\gtrsim$ 1 ns
• Pulse energy	200-1000 kJ
• Pulse repetition rate	10-1 Hz
• Average power	1-10 MW
• Overall efficiency	> 1%

These requirements on laser parameters have evolved and undoubtedly will continue to evolve, reflecting new knowledge in target and laser physics, materials and laser engineering, systems analysis and economics. Important constraints are encountered in each of the physics, technology and systems areas. For example, in the case of the laser wavelength, the physics constraints lead one toward short wavelengths to efficiently compress the pellet. A short wavelength requirement leads to investigation of laser transitions between electronic energy states. However, the materials and technology constraints force us to consider only wavelengths larger than $\sim$ 250 nm due to severe 2-photon optical absorption effects in lenses and windows. Operation with short wavelength also impacts the system and economics constraints because the short wavelength high average power lasers we know today are somewhat less efficient than infrared lasers. For each laser parameter there is a similar balance and interplay between the physics, technology and systems constraints, which often seems to leave very little room in parameter space to realize an acceptable solution. This study begins the problem-finding process involved in the conceptualization of full-scale systems, using a promising class of optically pumped gas lasers which appear to satisfy

the requirements listed above. We cannot say that the photolytic lasers considered in this study will indeed be the type to be developed to very large size, for much laser physics research yet needs to be done; but as a class, they adequately represent the pulsed power, e-beam, gas flow, chemical regeneration, optical quality and component damage problems characteristic of many high average power fusion laser systems. This allows the beginning of a fruitful assessment of the applicability of this technology to commercial power generation systems.

The laser media chosen for the first comparison study consists of atomic species radiating on electronic transitions, formed by photolytic dissociation from a parent molecule carried in a rare-gas buffer.[3,4] The four atoms of interest are oxygen, sulfur, selenium and iodine. The source of photolysis photons is the fluorescence from an 3-beam excited rare gas, possibly doped with another molecule to enhance fluorescence radiation in the absorption band of the molecule to be photolyzied. A companion study is being performed for laser-pumped photolytic lasers.

In Table I we list the features of photolytic lasers that recommend them for fusion power plants. These features include favorable target coupling characteristics, high energy storage per aperture, promising overall efficiency, and a choice of lasing atom and pump molecule combinations.

Figure 1 shows a possible configuration of a high average power photolytic laser system that appears very scalable to large volumes and high energy per pulse. The fluorescer gas and laser gas regions are kept apart by the stability of coflowing streams of different gases. The

pressure and velocity of the two gases are matched; the density, temperature, and Mach number generally will be different. This has the tremendous advantage of not requiring transmitting windows, which probably would not be able to withstand damage from high fluence levels of photons and 1-MeV electrons in addition to the steady and shock pressure loads over large spans (greater than 30 cm).

The configuration chosen is not the only possible photolytic laser. If a window can be found, allowing operation of the fluorescer gas at significantly higher pressure than the laser gas, or if an efficient UV laser pumped scheme can be devised, higher overall efficiencies may result. The flowing windowless fluorescer pumped geometry was chosen for this first study because we have substantial information on fluorescer efficiency but not on rare gas laser efficiencies. Furthermore, the configuration is demonstrably scalable to high average power. Comparisons between calculated efficiencies for different laser atoms will be more important than the absolute levels. Additional improvements in efficiency will no doubt come through future innovation in pumping configuration.

The lasing sequence is begun by the firing of two opposed $\sim$ 1-MeV e-beams for approximately 1 μs. In the case of the selenium laser sketched in Fig. 1, electrons radiolyze the xenon, resulting in copius xenon excimer (Xe_2^*) fluorescence radiation. The lasing medium consists of approximately 3×10^{16} cm^{-3} of COSe in 1 atm of helium buffer gas, which provides a pressure match to the fluorescer gas and provides sufficient heat capacity to minimize the increase in gas temperature.

TABLE I FEATURES OF PHOTOLYTIC LASERS

1. Choice of system:

Lasing atom	Lasing wavelength, nm	Parent molecule	Fluorescer excimer	Fluorescer wavelength, nm
Iodine	1130	C_3F_7I	$XeBr^*$	280
Oxygen	558	N_2O	Ar_2^*	130
Sulfur	772	COS	Kr_2^*	150
Selenium	489	COSe	Xe_2^*	170

2. Favorable target coupling characteristics:

   - WAVELENGTH: $\lambda = 0.5 - 1.3$ μm
   - SHORT PULSE DURATION: $\tau \sim 1 - 10$ ns

3. High-energy storage:

   - $F_{saturation} \sim 1\text{-}10 J/cm^2$

4. Favorable scaling characteristics:

   - Configurations allow flowing, high-average-power systems.
   - Can use low-pressure ($\sim$ 1 atm), low-temperature ($\sim$ 300 K), low-index gases (e.g. helium) for good beam quality.

5. Efficiency $\geq$ 1% possible from the physics.

FLOWING WINDOWLESS GEOMETRY

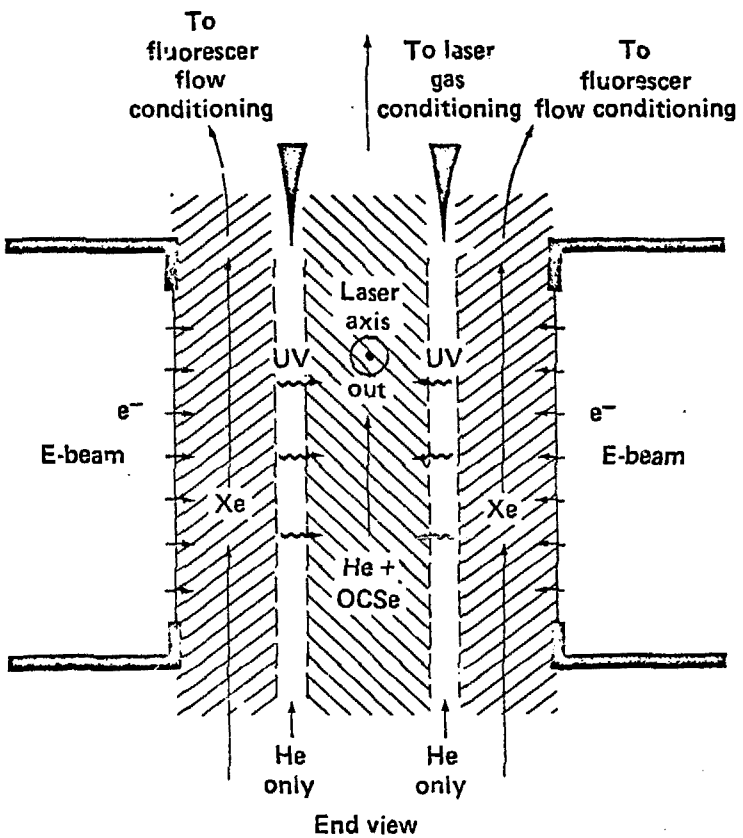

4/77

Figure 1

The fluorescence radiation dissociates the parent molecule; the resulting excited Se^* atom stores the energy long enough to achieve a high-energy storage fusion amplifier.[5]

The molecular absorber is optically thick to the fluorescence radiation. The photolysis occurs by a bleaching wave that is driven into the medium, dissociating the molecule and causing the mixture to become transparent. The sequence ends with injection of a 1-ns laser pulse that causes the medium to depopulate during amplification. The O^* & S^* laser systems operate similarly, but the iodine system is pumped in an optically thin manner.

The laser cavity configuration shown in Fig. 1 is a classic scalable geometry with the pump, flow, and optical extraction axes mutually orthogonal. This is a convenient way to decouple these important processes and reach the largest possible sizes based solely on constraints of the individual processes.

There are two very important and separate aspects to a large laser system: efficiency and scalability. A laser system of high efficiency will have lower recirculating power needs and lower capital equipment costs. The efficiency depends on the losses due to power conditioning, fluorescence production, coupling to the laser molecule, optical extraction, and pumping, cooling, and chemical regeneration of the flowing gases. On the other hand, a laser built with a large single aperture size and energy per pulse lowers costs by reducing complexity in the

number of beams and components. The scalability depends on optical and e-beam foil damage limits, pump constraints, flow and gas uniformity constraints, parasitic suppression, thermal distortion of optical elements, and a configuration that simultaneously pushes all the important technology barriers.

In any given laser system it is often possible to trade off efficiency versus scalability to achieve an optimal system. We discuss both these important aspects for the class of fluorescer-pumped photlytic lasers.

Efficiency

Fig. 2 is a power flow diagram of a photolytic laser system. Electrical power is taken continuously from the power plant's generating system for the electrical power conditioning (P_{EPC}), for the fluorescer gas conditioning (P_{FGC}), and for the laser gas conditioning (P_{LGC}). The laser system output is the laser radiation focusable on target, P_0. The overall laser system efficiency is then:

$$\eta_{LS} = \frac{P_0}{P_{EPC} + P_{FGC} + P_{LGC}} . \qquad (1)$$

which can be rewritten as

$$\eta_{LS} = \left(\frac{P_0}{P_L}\right)\left[\frac{1}{\frac{P_{ELC}}{P_L} + \frac{P_{FGC} + P_{LGC}}{P_L}}\right]$$

$$= \frac{\eta_0}{\left[\frac{1}{\eta_{ES}} + \frac{1}{\eta_{FS}}\right]} \qquad (2)$$

The laser system efficiency is effectively the product of the optical train efficiency and a parallel combination of the electrical or flow subsystem efficiencies.

The optical system efficiency is simply the ratio of the power on target divided by that emerging from the final laser aperture, accounting for losses in the optical transport system required to get the beam into the reactor building and focused on target. These losses include absorption and scattering of lenses and mirrors, as well as beam-shaping and diffraction-spillage losses. A typical optical train might require ten optical elements. We have assigned a value of 95% to this optical efficiency.

The electrical system efficiency is the ratio of laser radiation produced to electrical power provided to the pulse-forming network. It is the product of the pulse-forming network, e-beam, fluorescer, coupling geometry, quantum, and extraction efficiencies, as follows:

$$\eta_{ES} = \eta_P \eta_{EB} \eta_F \eta_C \eta_Q \eta_{EX}. \qquad (3)$$

In Table II, these efficiencies are estimated for the four candidate photolytic lasers. A range of values is given for the component efficiencies of each laser; the lower figure represents today's technology whereas the upper figure is a reasonable number believed achievable with future development. The larger number in a sense represents the best that can be envisioned for the configuration assumed in Fig. 2; further innovation would be needed to improve substantially on these estimates. Because we are projecting efficiencies of a laser system to be built 20 years hence, only the optimistic numbers are given for the total electrical efficiencies.

The fluorescence efficiencies can be derived from the product of the intrinsic fluorescence efficiency of the gas (40 to 50% for the rare gases, 15% for XeBr in Ar,[6,7,8]) and a geometrical factor to account for the loss of fluorescence radiation not directed at the laser medium (15 to 40%). The lasing efficiency is the product of quantum efficiency and the extraction fraction determined from the level degeneracies.

Two conclusions are immediately apparent from Table II. The selenium laser is superior because its quantum efficiency is 50% higher than those of the other Group VI atoms. This is due, in turn, to operation on the transauroral line rather than the auroral line. This is not likely in the oxygen or sulfur systems because of the greater gain of the auroral transitions in these atoms. We would like to operate the sulfur laser on the transauroral line for higher quantum efficiency, but the size is then limited by the fact that the amplifier must be sized to stand off the gain on the auroral line, which is 15 times greater.

Parameter		Efficiency, Percent			
		Oxygen	Sulfur	Selenium	Iodine
Pulse Forming	η_P	80 - 90	80 - 90	80 - 90	80 - 90
E-beam Diode & Foil Holder	η_{EB}	75 - 80	75 - 80	75 - 80	75 - 80
Intrinsic Fluorescence	η_F	40 - 50	40 - 50	40 - 50	10 - 15
Fluorescence Geometric Coupling	η_C	15 - 40	15 - 40	15 - 40	15 - 40
Quantum Efficiency	η_Q	20	19	35	21
Extraction Efficiency	η_{EX}	83	83	75	67
Total Electrical to Laser Efficiency	η_{ES}	0.6 - 2.4%	0.6 - 2.4%	0.95 - 3.8%	0.13 - 0.61%

TABLE II: Electrical to Laser Efficiencies for Photolytic Lasers

LASER SYSTEM POWER FLOW

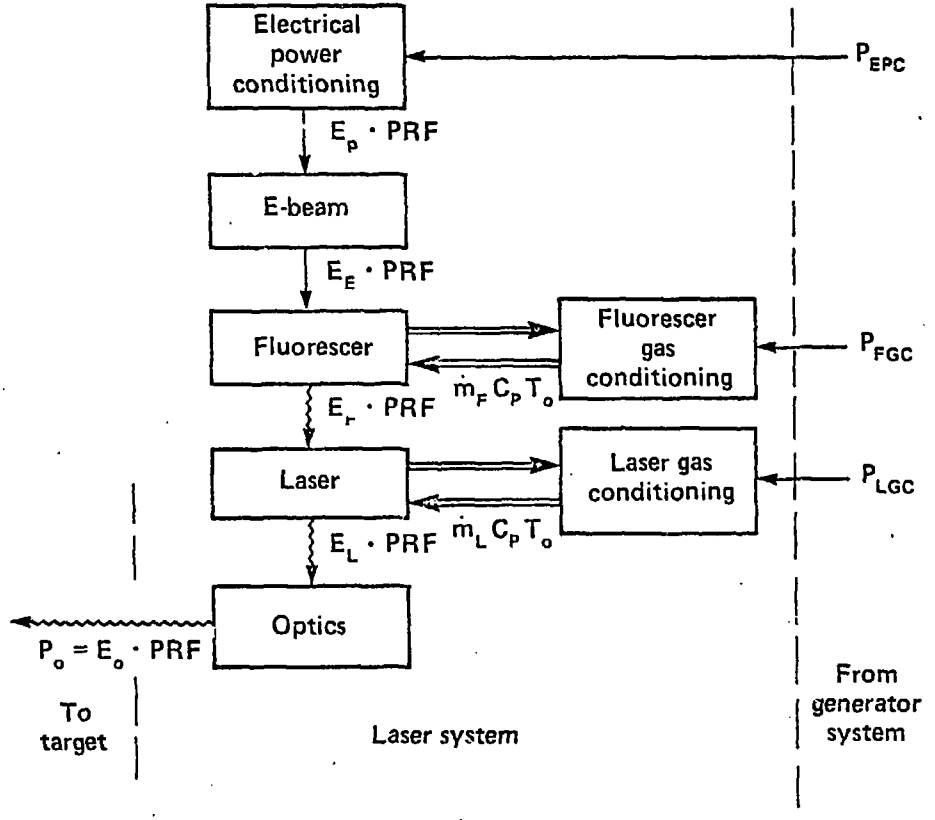

Figure 2

The net result is a higher overall efficiency but in an amplifier having more than an order of magnitude smaller energy output per aperture.

The iodine laser seems inferior for two reasons. First, the match between the $XeBr^*$ fluorescence band and the C_3F_7I absorption band is not nearly as close as for the Group VI atoms, resulting in two to three times lower fluorescence efficiency. Second, the quantum and extraction efficiencies are not as favorable. For example, the degeneracies in the iodine levels at best allow for only 67% extraction of the inverted population compared with 75 to 83% for the Group VI atoms. We shall see whether the factor-of-6 advantage of selenium over iodine worsens when flow efficiency is taken into account.

The flow system efficiency is simply

$$\eta_{FS} = \frac{P_L}{P_{FGC} + P_{LGC}} \tag{4}$$

The required fluorescence and laser gas flow conditioning powers are of two kinds. The first is the pumping power needed to make up stagnation pressure losses (entropy generation) due to screens and flow straightners, friction in the heat exchanges required to cool the flow, the laser heat addition itself, acoustic absorbers, and the like. This loss is proportional to the power of the circulating flow.

The second need for power is for chemical regeneration of the parent molecule in the laser process. Although this is proportional to the original number density of parent molecules, it is otherwise very

dependent on the chemical engineering details. The COS and COSe systems are the simplest because there appears to be a good chance to get the $2CO + S_2 = 2COS$ type reaction to occur, perhaps with a catalyst, requiring only enough additional power input to achieve vaporization of the condensed sulfur or selenium. On the other hand, the N_2O and C_3F_7I molecules dissociate into a host of compounds which require a complex and energy intensive regeneration process, making the O^* and I^* lasers much less attractive. As an example, a 1 MW average power laser system with a volumetric efficiency of 10 joules per liter of laser gas (helium plus a tenth percent by number of parent molecule) would require a process plant to recombine $\sim 2.7 \times 10^4$ kg/day of laser molecule. Of course the process plant must first separate the parent molecule from the stream of 9×10^6 liters/day of helium in order not to overload the regeneration process with all that inert gas. Clearly we must devise a method to recombine the parent laser molecule "on the fly," in some energetically favorable process such as simple heat addition in the presence of a surface catalyst. Because our estimates of these regeneration losses are not yet firm, we omit them from the analysis. We must keep in mind that these losses, particularly for the iodine laser, could be quite large.

Returning to the required pumping power, the power required for the two gas streams is proportional to the circulating power, which is the product of the mass flow, $\dot{m}$, and enthalpy $[C_pT_0 = C_pT + u^2/2]$:

$$P_{FGC} + P_{LGC} = \left[\xi_F \dot{m}_F + \xi_L \dot{m}_L\right] C_pT_0 \quad . \tag{5}$$

The constants ξ are the pumping efficiencies, which are function of the pressure drops or pressure ratios and are calculated from classical wind-tunnel formulae. Low-pressure-drop flow nozzles can be used in the

fluorescer gas stream because flow quality is not important. Let us assume that a wind tunnel with $\Delta p = 0.41$ atm (6 psi) can be designed for the fluorescer gas loop. The laser gas must have exceptionally uniform density to assure that fluctuations of the index of refraction are minimized. This requires a set of small, choked flow nozzles and screens with a high pressure drop, say $\Delta p = 2$ atm, or a pressure ratio of 3. The flow efficiencies that correspond to these pressure drops[9] in helium are $\Delta p = 6$ psi, $\xi_f = 0.20$ for the fluorescer gas loop and $\Delta p = 30$ psi, $\xi_L = 0.55$ for the laser gas loop. The two coflowing streams have the same velocity and pressure (~ 1 atm) in the laser cavity.

The flow efficiency expression for two streams is then,

$$\eta_{FS} = \frac{1}{\left(\frac{2\gamma}{\gamma-1}\right)\left[\frac{\xi_F W_F}{W_L} + \xi_L\right] \frac{p}{\eta_{ex} h\nu N^*}} \qquad (6)$$

where p is the gas pressure, γ the ratio of specific heats, W the widths of the fluorescer (F) and laser (L) streams, $h\nu_L N^*$ is the energy stored per unit volume in excited states and η_{ex} is the fraction of stored energy that can be extracted.

The flow efficiency depends on the relative sizes and pressure drops of the two streams and on the ratio of overall pressure to

excited-state density (more precisely, on the ratio of transitional energy density to the extractable energy density of excited states). Obviously it is desirable to operate at low helium pressure and high lasing molecule density. Note that the flow efficiency is independent of cavity volume or pulse repetition frequency, so long as the laser is operated at the minimum mass flow.

The flow system efficiency calculation depends on the results of the scaling relationships we are about to discuss, such as the relative widths of the laser and fluorescer streams, the pressure (1 atm) and the parent molecule number density. However, in order to keep the discussion of efficiency self contained, we give the results of the flow efficiency calculations in Table III for the four lasers of interest, exclusive of any chemical regeneration losses. The electrical and optical efficiency losses are repeated in this table in order to display the overall efficiency computed in Eq. 2.

The pressure drop given above for the laser gas is a conservative number, assuming that choked flow is absolutely required to prevent upstream propagation of acoustic waves generated in the pulsed laser cavity. It is quite possible that our pulse repetition rate is sufficiently low (1-10 per second) that we have a long enough clearing time between pulses to attenuate these waves in a low pressure drop cavity, say $\Delta p = 6$ psi, as is used in the fluorescer loop. This would have the effect for raising the flow efficiencies approximately 50%, although it depends on the ratio of the widths of the two different gas regions.

TABLE III: OVERALL LASER SYSTEM EFFICIENCIES FOR WINDOWLESS FLUORESCENCE-PUMPED PHOTOLYTIC LASERS

Subsystem		Efficiency, Percent			
		Oxygen	Sulfur	Selenium	Iodine
Electrical	η_{ES}	2.4	2.4	3.8	0.61
Flow	η_{FS}	0.40	1.1	2.8	0.2
Optical	η_o	95.	95.	95.	95.
Overall Laser System Efficiency $\eta_{LS} = \frac{\eta_o}{\left(\frac{1}{\eta_{ES}} + \frac{1}{\eta_{FS}}\right)}$		0.33%	0.72%	1.53%	0.14%

We immediately note that the flow efficiencies significantly influence the overall efficiencies. Because the fluorescer flow and laser flow must be pressure-matched in a windowless system, one must operate at a high enough total pressure (and therefore mass flows) to stop the e-beam efficiently in the fluorescer flow region. This makes it difficult to reduce the total pressure much below the assumed value of 1 atm. In addition, the oxygen and iodine lasers use argon, a relatively low-atomic-weight fluorescer which requires a much greater width of gas to stop the electrons; they therefore have a concommitantly larger pumping power requirement.

Scaling Considerations

Four factors dominate the sizing of photolytic lasers: parasitics, beam quality, e-beam foil damage, and the upper state lifetime. We have taken these factors into account in an analysis of the feasibility of constructing >100 kJ pulse amplifiers. The results are encouraging; it appears that it will be less difficult to obtain size than efficiency.

Parasitic oscillations must be suppressed in large laser amplifiers to prevent unwanted premature depopulation of the excited states. In the laser direction, it is quite likely that saturable absorbers will be used to isolate amplifier stages and prevent target preheating. This allows the use of high-gain-length products, particularly if aerowindows rather than solid windows are used, for they obviate the back-reflection problem. Consequently, we shall take a small signal gain-length product $g_0 L = 6$ as our parasitic limit on maximum length, a large but not unreasonable limit.

Parasitic oscillations must also be prevented in the two transverse directions. The flow direction is bounded in the upstream direction by a nozzle wall that may reflect light. However, the downstream direction is bounded by an aerodynamic diffuser full of hot absorbing gas, so we would anticipate no reflected radiation. In the pump direction, the laser cavity is bounded by fluorescent gas regions, which may or may not be transparent to the laser radiation depending on the ion density in the fluorescing gas. If they are transparent, the laser radiation could reflect off the e-beam foils, which have some reflectivity in the visible spectrum. If we never let the width of the laser gas exceed one-half of the length, we should avoid transverse parasitic problems.

There are other limitations on the width in the pump direction, such as quenching of the excited states of the photolyzed gas by the parent molecule during the pump pulse. The population inversion of the laser gas is prepared by the dissociation induced by absorption of the fluorescence radiation, but since the laser gas region is considerably larger than the characteristic absorption depth, it is optically thick to the fluorescence radiation. As the absorbing molecule dissociates, however, it cannot absorb again, causing the gas to become transparent or "bleach." Thus a bleaching wave propagates into the laser gas leaving behind excited metastable upper states of the laser transition, the lifetime of which is determined by collisional deexcitation, natural spontaneous emmission, or

stimulated emission, whichever is dominant. The radiative lifetimes of these metastable states are long (> .1 sec) so collisional quenching is of primary concern. This limit can be overcome to some extent by pumping harder for shorter times, thereby transferring a kinetics problem associated with the speed of the bleaching wave and the width of the absorber region into one of e-beam foil damage (F_E) limit of 20 J/cm^2, corresponding to 20 A/cm^2 for 1 ns or 200 A/cm^2 for 0.1 μs at electron energies of ∿ 1 MeV. The bleaching-wave velocity is simply the fluorescent photon number flux divided by the absorber (parent molecule) density. With an e-beam fluence limit of 20 J/cm^2, a bleaching wave can be driven approximately 120 cm into a gas with 3 x 10^{15} absorbers per cm^3. This result is relatively independent of the pumping time, which can be chosen to minimize quenching problems. Unfortunately, if one pumps too hard for short pump times, the fluorescence efficiency of the rare gases falls off to values less than 40% due to processes such as excited-state photoionization.

Mirror damage limits are not really of concern in this example because for a given energy stored and a given fluence constraint for the onset of mirror damage, say 10 J/cm^2, we can adjust the input fluence to the saturated amplifier to get the correct damage-limited fluence, since the saturation fluences of the media are in the 1 J/cm^2 range.

Beam quality is an important constraint, particularly for visible gas lasers in which the optical path variations can be significant. The chief sources of phase degradation for the coherent beam are density fluctuations in the gas which cause nonrandom linear fluctuations in the index of refraction, and the surface finish and thermal distortion of mirrors.

Each optical component is allowed part of an overall distortion budget, calculated from the greatest beam-quality loss that can be tolerated while still focusing on a fusion target. As an example, we performed the following linearized analysis.[10] Assume that the optical train needed for interfacing with the fusion reactor is composed of 10 mirrors, the last of which is a 2-m-diam focusing mirror. This final mirror is located 100 m from the center of the target chamber so as to minimize the chamber's open wall area, through which neutrons can escape. Each mirror is polished or diamond-turned to within $\lambda_v/10$ or $\lambda_v/20$ optical quality. The beam quality criterion is the capability to focus to a 1-mm spot.

The gas laser amplifier is assumed to have an input beam of zero phase variance and a minimum level of local gas density variation ($\Delta\rho/\rho$) due to flow noise of 10^{-3}. This level is the minimum yet achieved in a laser cavity, although 5×10^{-4} might be reachable. Helium is used as the buffer gas since argon would produce 7.5 times more fluctuation in the index of refraction than helium at the same average density and density-fluctuation level. Krypton and xenon, anywhere near 1 atm, would be unuseable; the allowed pressure of the heavier rare gases can be scaled from the helium curve (Fig. 3) by the ratios of the linear index of refraction minus one (n-1).

In Fig. 3 the results are given in terms of the product of gas pressure and length of the optical cavity in the lasing direction. This product is a function of laser wavelength, of course, because it is the optical-path difference compared with a wavelength that is the important factor in the loss of coherence. In helium at 1 atm, we are allowed about 5 m of amplifier length for the selenium laser whereas, at the larger iodine wavelength, a 15 m cavity might be tolerated. This simple example is only illustrative; we are now quantifying these considerations with physical optics calculations. Nevertheless, the general scaling relationships and parameter magnitudes are consistent with knowledge gained on large pulsed, flowing CO_2 lasers. Unfortunately, our belief that $(\Delta\rho/\rho)$ is relatively independent of the steady density level is based on data over a very small dynamic range, since few flowing lasers have the necessary path length to produce reliable data at 1 atm pressures.

The parasitic and beam-quality limitations on length are combined in Fig. 4 as a function of lasing molecule density. The beam quality, determined by the total gas pressure and index of refraction, sets the length; the parasitic limit sets the maximum lasing molecule density.

The length, height, width and number density considerations may be combined to calculate the maximum storable energy per amplifier module, i.e., in a single aperture. This is shown in Fig. 5. Oxygen, the system with the lowest gain, stores the greatest energy because these systems -- limited in both flow length and laser length by gain

BEAM QUALITY CONSTRAINT

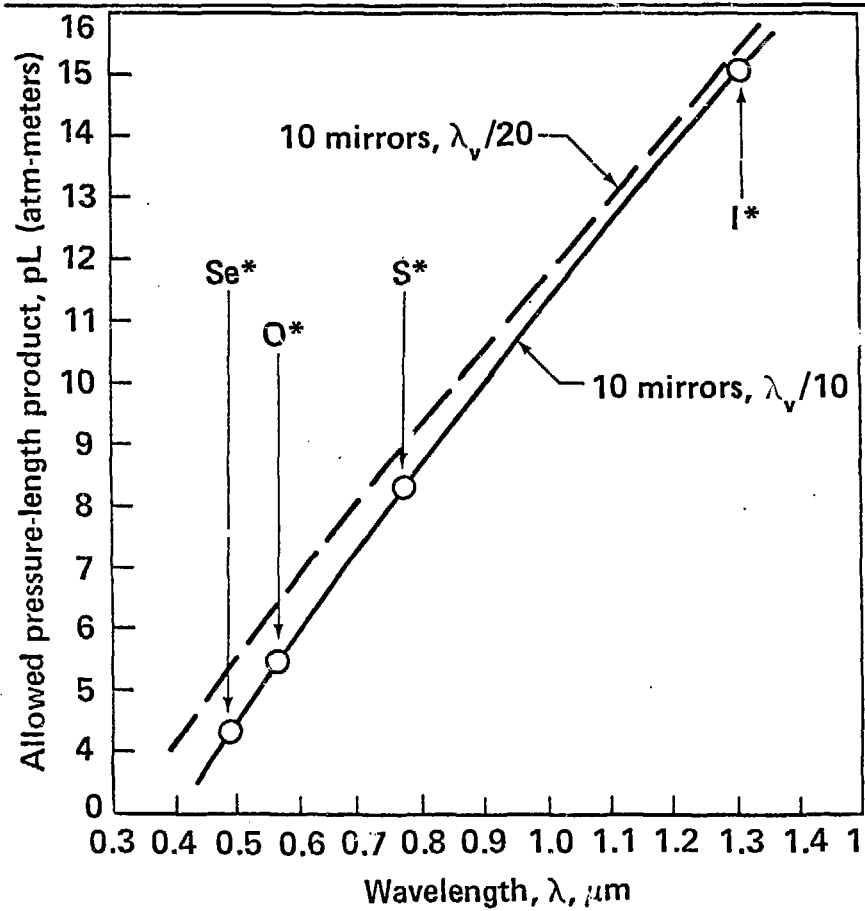

$\frac{\Delta\rho}{\rho} = 10^{-3}$ in pure helium

Focusing Criterion	1 mm
Focusing mirror	2 m
Mirror distance	100 m

4/77

Figure 3

LENGTH (LASING DIRECTION) CONSTRAINTS

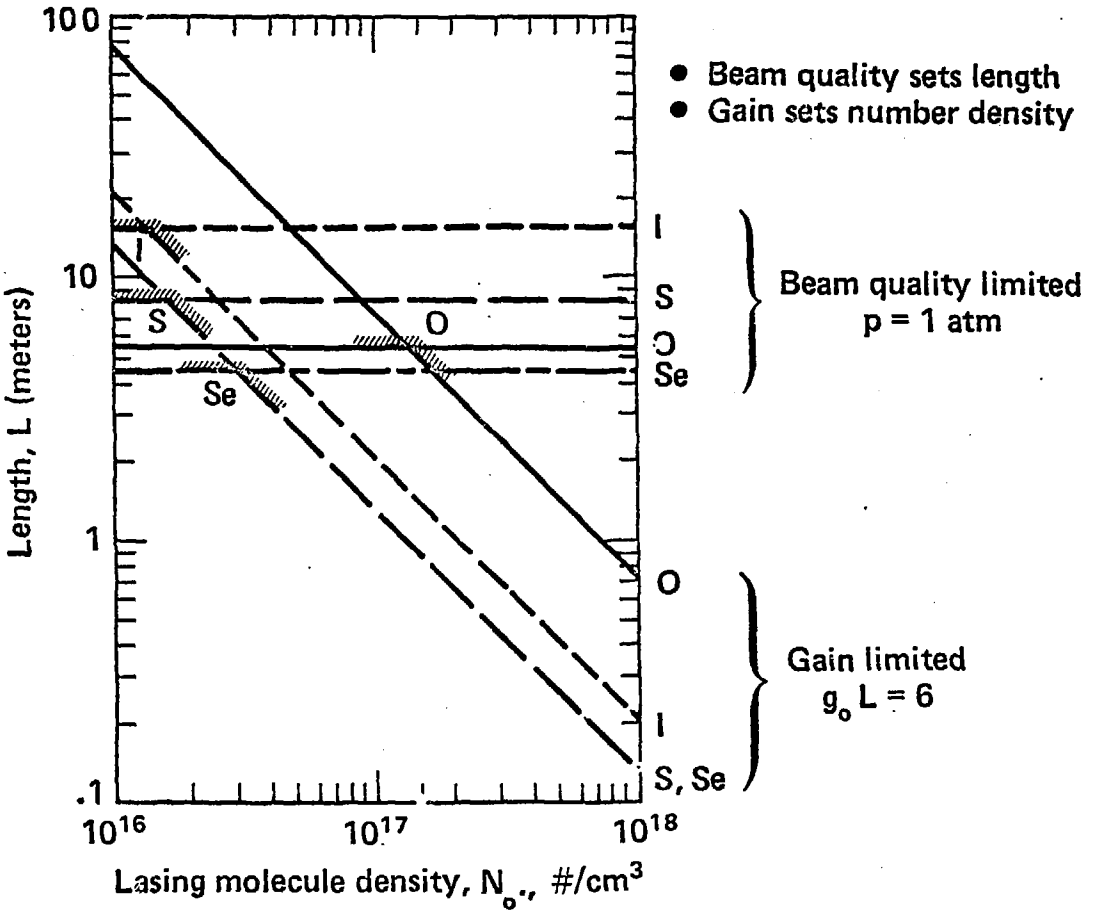

Figure 4

4/77

constraints -- store more energy per module by reducing the lasing molecule density and increasing the volume by a proportionately greater amount. In fact, only the oxygen system can store more energy than can be extracted, because of a mirror-damage fluence threshold of 10 J/cm^2. Consequently, for the oxygen-system curve in Fig. 5 only number densities less than about 8×10^{16} (to the left of the mark) represent extractable energies.

Conclusions to the Comparison Study

Using the specific case of a fluorescer-pumped windowless geometry to compare four high-average-power photolytic laser systems, we have determined that

a) Amplifiers may be built large enough to achieve 1 MJ with less than a dozen beams

b) Efficiencies above 1% are possible from the physics but are highly configuration dependent.

The selenium system offers the highest efficiency.

c) The iodine system, although the most highly developed photolytic laser, requires a tenfold higher power input than selenium. This is economically quite unfavorable.

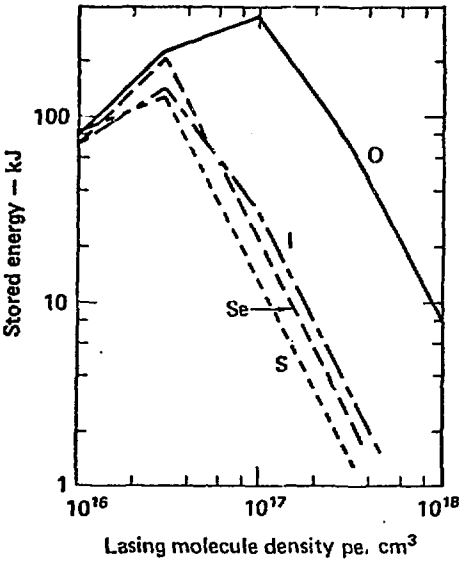
100
10
1
Stored energy — kJ
O
I
Se
S
10^{16}
10^{17}
10^{18}
Lasing molecule density pe. cm^3

Figure 5

Since the selenium system appears most promising, let us take a closer look at the scaling relationships to see if overall efficiency can be improved by some optimization of a 125 kJ amplifier module.

A Selenium Laser System for a Commercial Power Plant

In this section we present a summary of the parameters of a photolytic selenium laser system, using the same basic windowless configuration. We have realized increased efficiency through improving the flow efficiency, designing for exactly a 125 kJ size, and taking advantage of the size and shape scaling with gas pressure. The laser cavity works in exactly the same way as before, with the laser gas bounded by two flowing "flashlamps" with no window in between. The only change is one of size and energy density; a small high-excited-state density cavity will have a greater laser output per unit volume and a lower required flow power requirement. This will allow a higher flow efficiency and an overall laser efficiency of 2%, which appears to be the limit for this configuration.

The laser output per unit volume may be expressed as

$$\frac{E_L}{\text{Volume}} = \eta_{ex}\, h\nu\, N^*$$

where η_{ex} is an extraction efficiency, $h\nu$ is the energy per photon and N^* is the population inversion density. The maximum population inversion can be increased and the volume decreased by increasing the gas pressure as described below.

The length of the laser is constrained by beam quality to have a constant pressure-length product, so that the length of the laser is inversely proportional to pressure. If we then operate at a constant gain length product

$$g_o L = \sigma N^* L = 5$$

with a pressure-broadened stimulated emission cross section (which is also inversely proportional to pressure) the maximum allowed population inversion will then scale as the square of the pressure, $N^* \sim p^2$. Thence, by increasing the pressure to 2 atmospheres we can halve the laser length and quadruple the allowed population inversion. Since the flow efficiency is directly proportional to N^*/p, the efficiency will be improved by a factor of two.

Of course the transverse dimensions will also be affected. A consistent set of values for all the important parameters is given in Table IV for one 125 kJ amplifier module. Eight modules in parallel are required to obtain a 1 MJ per pulse, 1.4 MW average power commercial system. Two additional standby modules are included for redundancy and reliability.

The gas velocity in each laser cavity is 5.5 m/s, sufficiently fast to allow a pulse repetition frequency of 1.4 per second. Between pulses the gas moves a distance equal to 1.5 cavity lengths.

The mirror fluence of 7.7 joules/cm^2 should not be excessive for 489 nm light, although the required mirror sizes are not small (75 cm x 240 cm).

The crucial technical issue in the feasibility of this conceptual design involves the long required pump times and high excited-state densities. The values given are quite optimistic and it is quite likely that in reality quenching near the fluorescer-laser interface, where the atoms are excited at the beginning of the pulse, would result in a very nonuniform transverse gain distribution.

Experiments are currently being conducted at LLL to determine the gain and excited state lifetime for the Group VI atoms; until these results are known it does not seem worthwhile to refine these numbers.

An accurate impression of such a full scale power plant driver is given in the artist's conception of Fig. 6. The middle floor contains the laser cavities, electron beams and pulse transmission lines. These are the large cylindrical energy storage devices extending out horizontally on each side. The flow systems, one for the (He + OCSe) flow and another for the xenon flow, are on the top floor. The bottom floor contains all the rectifiers, charging power supplies and electrical isolators. A key feature of the design is an optical tunnel which runs the entire length of the building and is vibrationally isolated from the laser building. All the mirror mounts are attached to the tunnel structure, isolated from the compressors and e-beam pulsing loads. The eight laser beams from the ten modules are generated in the vertical direction, turned in a right angle, and carried in beam tubes to the reactor.

Energy on Target	125 kJ	Optical Efficiency	95%
Energy out of Laser Module	139 kJ	Electrical Efficiency	3.5%
Pulse Repetition Frequency	1.4 Hz	Flow Efficiency	5.3%
Pulse Duration	1 ns	Overall System Efficiency	2%
Optical Cavity Volume	4.63 m^3	Volumetric Efficiency	15 J/ℓ-atm
Length in Beam Direction	2.55 m	Flow Velocity	5.5 m/s
Width in Flow Direction	2.4 m		
Width in E-Beam Direction	0.75 m		
Width of Each Fluorescer Region	0.35 m		
COSe Molecule Density	10^{17} cm^{-3}		
Pressure	2 atm		
Mirror Fluence	7.72 J/cm^2		
Saturation Fluence	2.24 J/cm^2		
E-Beam Fluence	13.1 J/cm^2		
E-Beam Voltage	1.25 MV		
E-Beam Current Density	6.8 $amps/cm^2$		

Table IV. Parameters of 125 kJ, 1.4 pps Amplifier Module

COMMERCIAL LASER FUSION POWER PLANT

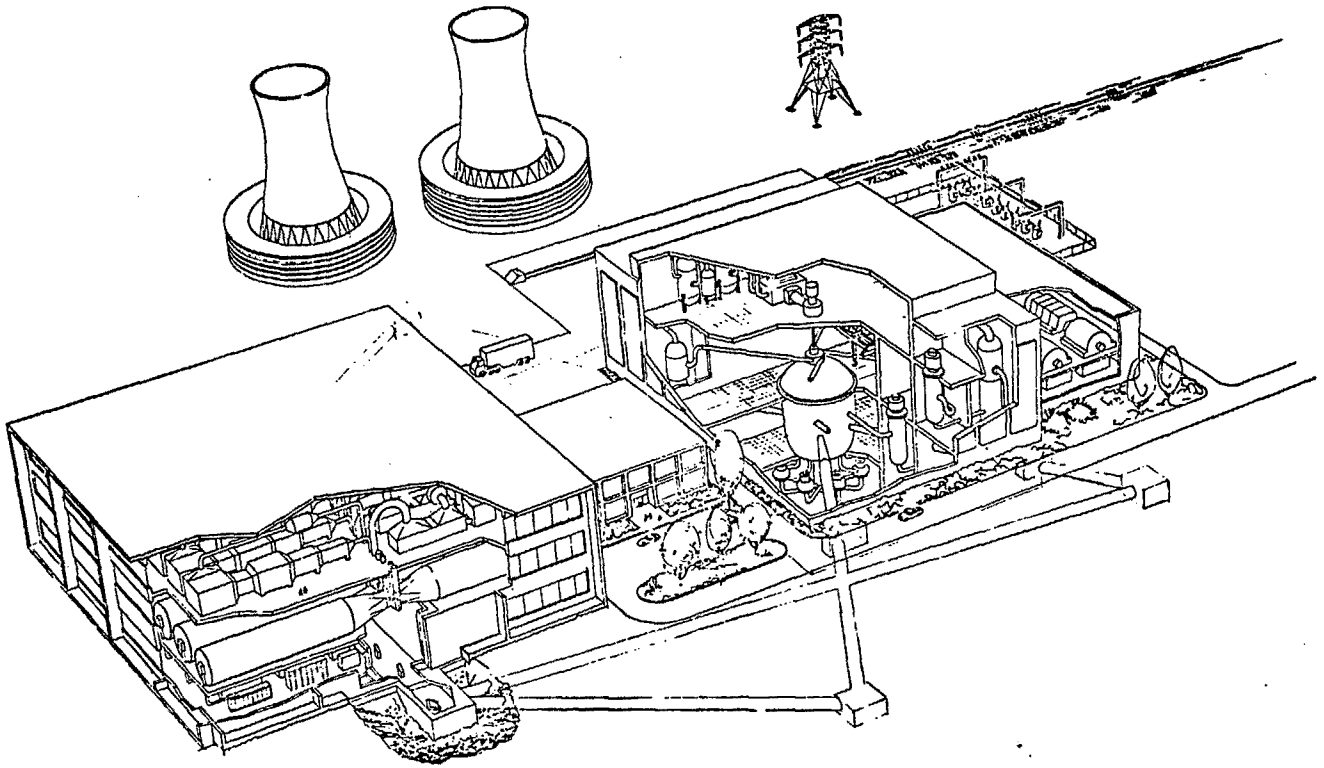

Eight beam total, four shown

Figure 6

Cost Considerations

It is premature to cost a particular 1 MJ visible laser system in detail because of the great uncertainties in the physics and technology of lasers which are still in the research stage. However, it is desireable to know approximately the capital cost of a laser system compared to the reactor system, and the expected sensitivity of cost as a function of major laser parameters such as pulse repetition frequency and overall efficiency. Usually estimates of relative cost and cost sensitivities are less dependent on the exact details of a laser system and have more general usefulness. For example, all gas laser systems in the 1-10% overall efficiency range will have costs which are dominated by the energy storage requirements and flow pumping and cooling requirements, relatively independent of the laser cavity and optical configuration.

An extremely approximate cost model was used to begin the process of balancing reactor operating parameters and costs against laser operating parameters and cost. For example, if we had estimates of how cost scales with pulse repetition frequency for both the reactor and laser, we could pick a system pulse rate which balanced the marginal savings for one system against the marginal increased costs of the other. This cost model simply breaks up the laser system direct capital costs into five categories:

1) energy storage and power conditioning
2) laser cavity and flow system
3) complete optical system
4) instrumentation and controls
5) building construction

We shall use the following nomenclature, where each quantity is per module.

C_i = direct capital cost for each category
η_0 = optical subsystem efficiency
η_{EC} = electrical conditioning efficiency
η_{FC} = flow conditioning efficiency
EC = energy input to electrical conditioning
FC = energy input to flow conditioning
E_L = energy out of final laser amplifier
E_0 = energy on target
N_0 = number of operating modules
N_S = number of spare modules (for reliability)
PRF = pulse repetition frequency
a,b = cost constants

Each cost category has a cost proportional to the energy per pulse and to the power consumed. This is required because some portions of the system depend on intrinsically pulsed phenomena and others on intrinsically continuous processes. We summarize the cost estimates as follows.

The cost of electrical conditioning is proportional to both the energy stored and the power dissipated (since cooling must be provided).

$$C_1 = a_1 E_{ec} + b_1 (1 - \eta_{EC}) E_{EC} (PRF)$$

$$= \left[a_1 + b_1 (1 - \eta_{EC}) PRF \right] \frac{E_L}{\eta_{EC}}$$

where

a_1 = 2.15 \$/joule stored

b_1 = 0.046 \$/watt dissipated

The cost per joule stored seems high compared to glass laser power system costs (.20 \$/joule) because the e-beams are included in our breakdown whereas flashlamps and associated hardware are usually excluded from the glass laser energy estimates. Furthermore, e-beams and pulse forming hardware are considerably more expensive for 1 μsec pump times than for 1 ms.

The cost of the flow system including compressors, piping, heat exchangers, laser cavity and chemical regeneration is proportional to the circulating power of the gases.

$$C_2 = \frac{b_2 E_L (PRF)}{\eta_{FS}}$$

where b_2 = 0.862 \$/watt input.

The cost of optics, optical bench structure, and alignment system (but without computer controls) is assumed to be proportional to the size of the mirrors (or energy incident for a given damage threshold) and to the power absorbed. This assumes about a dozen high average power mirrors at full aperture size (0.5 m x 2 m) per module.

$$C_3 = a_3 E_L + b_3 (1 - \eta_0) E_L \, PRF$$

where

a_3 = 9.0 \$/Joule incident

b_3 = 32.1 \$/watt absorbed

The instrumentation and controls are assumed to cost 7% of the hardware cost exclusive of the building. Hence the cost of instrumentation and controls is

$$C_4 = r_4 [C_1 + C_2 + C_3]$$

where $r_4 = 0.07$

The cost of the building is proportional to the energy storage and the power input to the flow system, because these parameters most affect the size of the building. Hence

$$C_5 = a_5 \frac{E_L}{\eta_{EC}} + \frac{b_5 E_L (PRF)}{\eta_{FC}}$$

where

$$a_5 = 0.64 \text{ \$/joule stored}$$

$$b_5 = 0.033 \text{ \$/watt input to flow system}$$

No contingency fee is included in this model. All the above costs are for a single module of the 10-100 kJ size. The total cost for N_0 operating pulus N_S standby modules is

$$C = (N_0 + N_S) \sum_i C_i$$

Remembering that the overall laser system efficiency can be written in terms of the subsystem efficiencies as

$$\eta_{LS} = \frac{\eta_0}{\frac{1}{\eta_{FC}} + \frac{1}{\eta_{FC}}},$$

the total power input to the laser system is as follows

$$P_{IN} = N_0 \frac{\eta_0 E_L (PRF)}{\eta_{LS}} = \left[\frac{1}{\eta_{EC}} + \frac{1}{\eta_{FC}}\right] N_0 E_L (PRF).$$

The most appropriate normalized cost is the direct capital cost per unit electrical power input. It is much less sensitive to the individual laser subsystem efficiencies and independent of overall laser system efficiency. Combining all the above formulae, the cost per input power, in dollars per watt, is:

$$\tilde{C} = \frac{C}{P_{IN}} = \frac{\left(1 + \frac{N_S}{N_0}\right)}{\left(\frac{1}{\eta_{EC}} + \frac{1}{\eta_{FC}}\right)} \left\{ \underbrace{\frac{2.3}{\eta_{EC}\,(PRF)} + 0.049\left(\frac{1}{\eta_{EC}} - 1\right)}_{\text{Electrical}} + \underbrace{\frac{0.922}{\eta_{FC}}}_{\text{Flow}} \right.$$

$$\left. + \underbrace{\frac{9.63}{(PRF)} + 34.3\,(1 - \eta_0)}_{\text{Optics}} + \underbrace{\frac{0.64}{\eta_{EC}\,(PRF)} + \frac{0.033}{\eta_{FC}}}_{\text{Building}} \right\}$$

The normalized cost is a function of five parameters: the three subsystem efficiencies, the pulse repetition frequency, and the redundancy factor. The costs for instrumentation and controls have been included into the electrical, flow and optics costs. Again, no contingency or escalation is included.

As a numerical example, the laser system described herein has the following efficiencies: $\eta_0 = 0.95$, $\eta_{EC} = 0.035$, $\eta_{FC} = 0.053$. This leads to an overall system efficiency of 2%. We have eight operating modules and postulate two standby modules so that $\left(1 + \frac{N_S}{N_0}\right) = 1.25$. The cost per unit input power can then be graphed as a function of pulse repetition frequency, as in Fig. 7.

The dominant conclusion is inescapable: It is most cost-effective from the viewpoint of laser capital cost to operate the laser at a pulse repetition rate of ≥ 5 Hz. Below this value the cost rises rapidly, and above this value there is diminishing returns. Increasing the pulse repetition rate from 1 to 5 will decrease

CAPITAL COST OF PHOTOLYTIC LASER SYSTEM

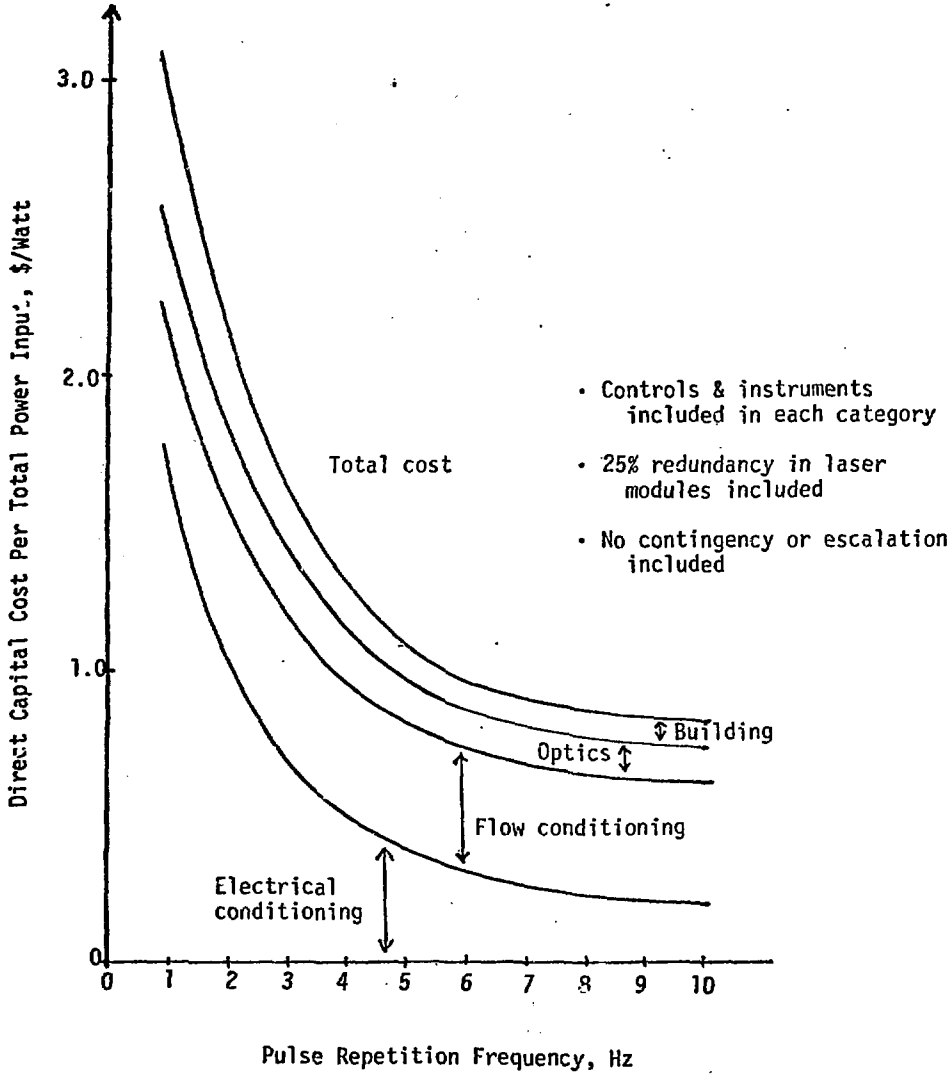

Figure 7

the laser system cost by a factor of 3. This is due to the high costs of energy storage, pulse forming units and electron beams per unit of stored energy, which decline rapidly as one operates at lower energy per pulse and higher gas flow rate (higher PRF). It remains to be seen how this affects the overall power plant cost and configuration.

Finally, the capital cost will vary exactly inversely with overall system efficiency. The incentives to obtain high efficiency laser systems which can operate at high average power, short pulselength and short wavelength are clear and strong.

Technical Issues

First, there are still great uncertainties in the laser kinetics, particularly in excited state-excited state quenching rates for sulfur and selenium. A high rate of self quenching of the upper level would lead to storage times shorter than expected. This would lead to shorter required e-beam pulse durations and smaller transverse dimensions. Perhaps a larger number of smaller modules would then be needed. Efficiencies should be less affected, however.

Second, large area (6 m^2) modular-diode e-beams of the type required are not yet available. We feel that they can be developed within the physics constraints, however, if the resources are made available.

Third, chemical regeneration costs and processes are still not known. The COS and COSe systems should be the least difficult and expensive, for it appears that heat addition in the presence of a catalyst may be sufficient. The iodine system, requiring a $i\text{-}C_3F_7I$ regeneration plant, appears to be formidibly costly and energy intensive.

Fourth, the effect of beam quality degradations in large laser amplifiers, particularly as it involves the ability to utilize low pressure drop laser cavities, is crucial for both length scaling and flow efficiency reasons.

Fifth, the overall efficiency of photolytic lasers is highly configuration dependent. A system using a window between fluorescer and laser (or perhaps a laser pumping scheme instead of the fluorescer) may offer factors of 2 in efficiency improvement. Successful configurational innovation will pay great dividends.

Sixth, rectangular mirrors of large size (~ 1 m x 3 m) be required.

Conclusions

1. A 100 kJ amplifier module appears feasible from standard laser scaling considerations. These may be operated at 1-10 pulses per second with appropriate closed cycle wind tunnels. Consequently, 1 MJ per pulse 1-10 MW modularized laser driver systems, operating at short wavelength and pulselength (1 ns) may be envisioned.

2. Efficiencies above 1% may be obtained, adequate to meet the present fusion requirements. The selenium laser offers the highest efficiency and the best chance to reach the 2-4% range, due primarily to the high quantum efficiency of the transauroral transition and the lower mass flows of rare gas (xenon) needed to stop the electron beam efficiently.

3. The configuration used in the study, using windowless fluorescer pumping, is a very conservative approach to scaling to large sizes, since it obviates the need for high strength, high transmission UV windows between the "flashlamp" fluorescer region and the laser gas. The technology risk would not be high.

4. The modularity of laser system allows use of spare modules which are being refurbished or kept ready for unscheduled breakdowns. This greatly enhances system reliability and availability.

5. The laser system would be separate from the reactor building and have an ordinary industrial outer structure. This is much less expensive than previously considered intra-reactor vessel concepts.

6. Pulse repetition rates of 1-10 Hz are no problem from power conditioning or optics viewpoints. Costs are a factor of 3 lower for 5 pps than for one pulse per second. Costs vary inversely with laser efficiency as expected.

In summary, photolytic lasers can meet the requirements for a commercial laser fusion power plant. They are still in any early research stage so the uncertainties in the physics are still large; but there is sufficient room for technical ingenuity within these constraints to develop an attractive high-average-power, short-wavelength gas laser system with reasonable efficiency.

Acknowledgements

The author would like to thank Drs. James Maniscalco and J. J. Ewing of Lawrence Livermore Laboratory for their technical insight and friendship, Brian Marais and Dr. Scott Thomson of Bechtel Corporation for their knowledge of process efficiencies and costs, and Audrey Heine for her cheerful, reliable and accurate support.

References

1. J. Nuckolls, "Laser Fusion Overview," presented at the Ninth International Quantum Electronics Conference,June 14-18, 1976, Amsterdam, the Netherlands. Also, Lawrence Livermore Laboratory, Livermore, CA, UCRL-77725 (May 17, 1976).

2. R. R. Buntzen and C. K. Rhodes, Laser Systems for Laser Fusion, Lawrence Livermore Laboratory, Livermore, CA, UCRL-75367 (1974).

3. J. R. Murray and C. K. Rhodes, "The Possibility of High Energy Storage Lasers Using the Auroral and Transauroral Transitions of Column VI Elements," J. Appl. Phys. 47 (1976).

4. K. Hohla and K. Kompa, "The Photochemical Iodine Laser," in Handbook of Chemical Lasers, R. W. F. Gross and J. F. Bott, Eds. (Wiley - Interscience, New York, 1976), p. 667.

5. J. J. Ewing, Lawrence Livermore Laboratory, Livermore, CA (December 6, 1976).

6. J. C. Swingle, C. E. Turner, Jr., J. R. Murray, E. V. George, and W. F. Krupke, "Photolytic Pumping of the Iodine Laser by XeBr," Appl. Phys. Lett. 28, 7 (1976).

7. G. Brederlow, K. J. Witte, E. Fill, K. Hohla, and R. Volk, "The Asterix III Pulsed High-Power Iodine Laser," IEEE J. Quantum Electronics QE-12, 2 (1976).

8. W.F. Krupke and E.V. George, "High Average Power, Rare Gas Halogen-Pumped Iodine Laser for Fusion Applications," Lawrence Livermore Laboratory, Livermore, CA, UCRL-77523 (1976).

9. H. W. Liepmann and A. Roshko, Elements of Gasdynamics (John Wiley & Sons, New York, 1957).

10. H. E. Bennett and P. C. Archibald, "Optical Requirements for Laser Mirrors," in Laser Induced Damage in Optical Materials: 1974, A. J. Glass and A. H. Guenther, Eds. (National Bureau of Standards, Washington, D.C., Special Publication 414, December 1974).